OL Organic Letters

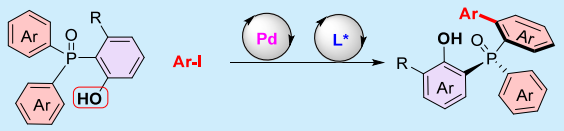
pubs.acs.org/OrgLett Letter

Palladium-Catalyzed Directed Asymmetric C−H Arylation Leading to a P-Stereogenic Center

Shengzhou Jin,*[,∇] Mohammad Khavani,[∇] Yu Wang,[∇] Ankit Pandey, Qiyang Jiang, Sai Zhang, Ruibin Liang,* and Guigen Li*

Cite This: *Org. Lett.* 2026, 28, 12587−12593 Read Online

ACCESS | Metrics & More | Article Recommendations | Supporting Information



- The first hydroxyl as directed group for P-stereogenic construct
- High ee and yields for most cases (up to 90% yield and 98% ee)
- Broad substrate scope (30 examples)

ABSTRACT: A novel -OH group-directed asymmetric catalytic C(sp^2)−H arylation has been developed, enabling efficient access to P-stereogenic chiral compounds with excellent yields (up to 90%) and enantioselectivity (up to 98% ee). The success of this C−H functionalization system relies on the synergistic coordination of a phenolic hydroxyl functionality and (*S*)-6-oxopiperidine-2-carboxylic acid with the Pd metal center, which acts as the efficient directing group and chiral ligand. The reaction demonstrated a broad substrate scope, affording a diverse array of 30 distinct P-chiral products. The absolute configuration of the products was unambiguously confirmed via X-ray diffraction analysis. Furthermore, a plausible catalytic cycle mechanism has been proposed, which is supported by detailed experimental studies and DFT calculations.

Chiral phosphorus compounds play an important role in catalytic asymmetric synthesis due to their dual utility both as chiral ligands for metal catalysts and as organocatalysts.[1] Ever since Knowles[2] first introduced P-chiral phosphines CAMP and DIPAMP for rhodium-catalyzed asymmetric hydrogenation nearly half a century ago, the development of various chiral phosphine ligands (Figure 1) has

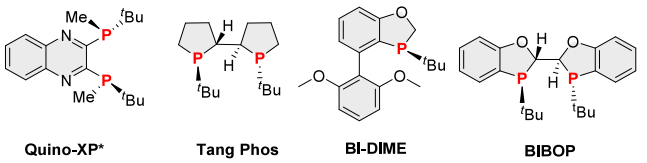


Figure 1. Examples of P-stereogenic centers.

been crucial to the rapid progress of asymmetric catalysis.[3] In order to improve the efficiency of the present transformations and discover new reactions, enormous chiral phosphorus compounds have been developed.[4] The construction of P-chiral compounds has primarily employed conventional optical resolution methods, and these processes typically depend on stoichiometric amounts of chiral auxiliaries. Beyond the use of chiral auxiliaries and resolution techniques, catalytic asymmetric methods have emerged as valuable synthetic strategies in recent years.[5] These approaches encompass a broad spectrum of transformations, including C−H activation, phenolic OH functionalization, alkyne diversification, allylic alkylation, phosphonoalkylation, arylation, amination, ring-closing metathesis, halogenative cyclization, hydroarylation, and hydrophosphination.

Directed C−H bond activation catalyzed by transition metals has emerged in recent decades as a powerful synthetic strategy.[6] Yu and co-workers have successfully demonstrated the versatility of this elegant strategy across various C−H activation modes.[7] Recently, the development of enantioselective C−H functionalization guided by directing groups has provided a practical route for the assembly of chiral molecules. In 2015, Han and co-workers[8] employed the Pd(II)/mono-N-protected amino acid (MPAA) catalytic system, developed by Yu's group,[9] to achieve enantioselective C−H activation directed by 2,3,5,6-tetrafluoro-4-cyanophenylamino (Ar^F) for the synthesis of P-stereogenic phosphonamides (Scheme 1a). Since then, numerous efficient catalytic systems have emerged for synthesizing P-stereogenic phosphorus compounds, leveraging diverse directing groups. In 2021, Ke and colleagues[10] developed an iridium-catalyzed, enantioselective *ortho* C−H boronylation protocol directed by phosphonate groups, enabling the construction of P-stereogenic phosphorus compounds (Scheme 1b). The resulting borylated chiral phosphinates exhibited versatile reactivity, undergoing diverse transformations at the C−B and P−O bonds, thus highlighting their potential as versatile intermediates for synthesizing functionalized P-stereogenic compounds. In the same year,

Received: August 1, 2026
Revised: September 9, 2026
Accepted: September 25, 2026
Published: September 29, 2026

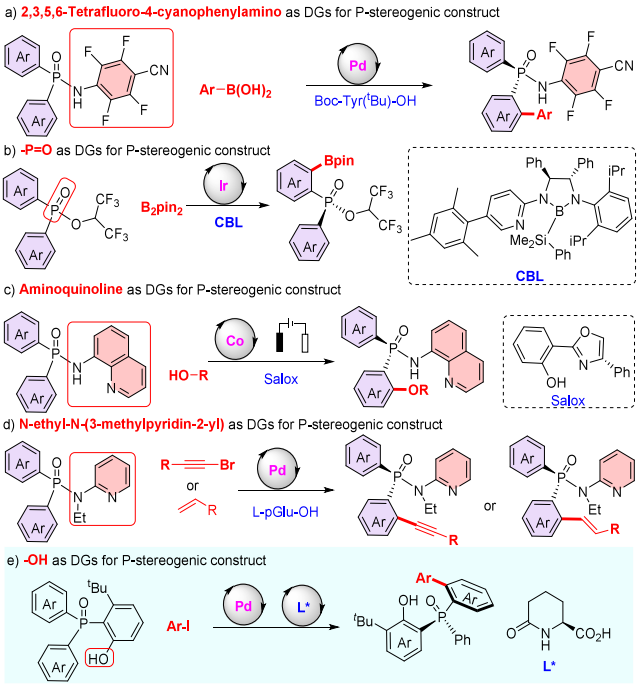


Downloaded from pubs.acs.org/orlef7/article-pdf/28/40/12587/6869849/acs.orglett.6c03398.pdf by TEXAS TECH UNIV user on 22 October 2026

© 2026 American Chemical Society

https://doi.org/10.1021/acs.orglett.6c03398
Org. Lett. 2026, 28, 12587−12593

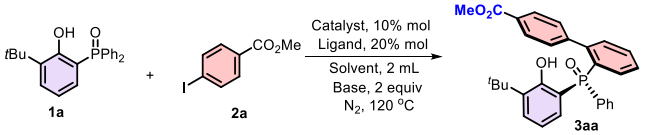
Scheme 1. Prevalent Research of Directed C(sp^2)−H Activation for P-Stereogenic Constructs



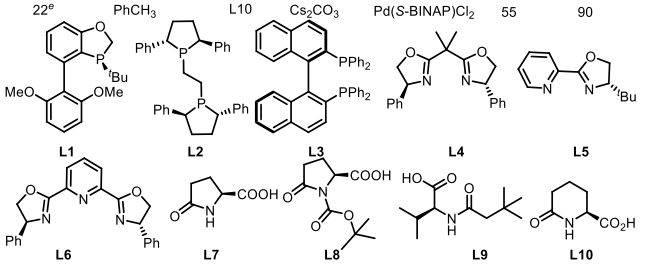
Li[11] reported a rhodium-catalyzed 1:2 coupling cyclization of diarylphosphinic amides and diarylacetylenes under mild conditions, directed by the phosphine oxygen group. This transformation proceeds via dual C−H bond activation, constructing biaryl frameworks that possess both central and axial chirality. In 2023, Shi's group[12] pioneered an electrochemical, Co(II)-catalyzed enantioselective C−H alkoxylation, efficiently synthesizing diverse enantioenriched alkoxylated phosphonamides with a high degree of stereocontrol by using 8-aminoquinoline as the directing group (Scheme 1c). Mechanistic studies revealed that an unusual Co(III) alcohol complex is a pivotal intermediate and that a base facilitates the Co(III)-to-Co(IV) oxidation, consistent with an operative Co(III/IV/II) catalytic cycle. At the same time, the groups of Zhou,[13] Ackermann,[14] and Sundararaju[15] also used 8-aminoquinoline as a directing group and successfully constructed various chiral compounds centered around phosphorus through an asymmetric C−H bond cyclization strategy. Subsequently, the Shi's group[16] continued to report on the enantioselective C−H alkynylation and olefination directed by *N*-ethyl-*N*-(3-methylpyridin-2-yl) amine, utilizing the Pd(II)/L-pyroglutamic acid catalytic system (Scheme 1d). The reaction proceeded through desymmetrization or kinetic resolution, providing direct access to diverse P-stereogenic phosphonamides with high enantioselectivity. However, existing asymmetric C−H activation strategies are often limited in substrate scope and rely on directing groups that are cumbersome to install and remove. Therefore, the development of new directing groups and efficient asymmetric C−H functionalization methods to access diverse P-stereogenic chiral compounds remains a valuable synthetic goal. Building on our previous work with palladium/amino acid catalytic systems for directed asymmetric C−H activation,[17] we now report a novel phenolic hydroxyl-directed asymmetric C−H arylation (Scheme 1e). This method offers an effective strategy to access P-enantiomeric chiral compounds, wherein hydroxyl groups serve as directing groups, a feature that has not been exploited in this context before. Using this approach, we successfully constructed a series of pentavalent phosphine derivatives, which we believe may lay a useful foundation for the future development of novel phosphine oxygen bidentate ligand libraries.

The model reaction was commenced by using **1a** ((3-(*tert*-butyl)-2-hydroxyphenyl)diphenylphosphine oxide) and **2a** (methyl 4-iodobenzoate) as the substrate. Initially, the reaction conditions included $Pd(OAc)_2$ (10 mol %) as the catalyst, Cs_2CO_3 (2.0 equiv) as the base, and BI-DIME (**L1**, 20 mol %) as the chiral ligand in cosolvents of $PhCH_3$ (2 mL) under an argon atmosphere. The reaction was conducted at 120 °C for 48 h, affording product **3aa** in 62% yield and 58% ee (Table 1, entry 1). Inspired by these outcomes, we continued to screen for different types of chiral phosphine ligands such as BINAP and Ph-BPE (Table 1, entries 2 and 3, respectively). Unfortunately, the results showed that compared to **L1**, these chiral phosphine ligands reduced the product yield and enantioselectivity to varying degrees. Several other chiral

Table 1. Optimization of the Reaction Conditions[a]



entry	Solvent	Ligand	Base	Catalyst	yield (%)[b]	Ee (%)[c]
1	$PhCH_3$	L1	Cs_2CO_3	$Pd(OAc)_2$	62	58
2	$PhCH_3$	L2	Cs_2CO_3	$Pd(OAc)_2$	58	51
3	$PhCH_3$	L3	Cs_2CO_3	$Pd(OAc)_2$	40	64
4	$PhCH_3$	L4	Cs_2CO_3	$Pd(OAc)_2$	31	25
5	$PhCH_3$	L5	Cs_2CO_3	$Pd(OAc)_2$	45	18
6	$PhCH_3$	L6	Cs_2CO_3	$Pd(OAc)_2$	33	36
7	$PhCH_3$	L7	Cs_2CO_3	$Pd(OAc)_2$	48	55
8	$PhCH_3$	L8	Cs_2CO_3	$Pd(OAc)_2$	39	40
9	$PhCH_3$	L9	Cs_2CO_3	$Pd(OAc)_2$	27	59
10	$PhCH_3$	L10	Cs_2CO_3	$Pd(OAc)_2$	44	76
11	$PhCH_3$	L10	Cs_2CO_3	$Pd(PPh_3)_4$	52	16
12	$PhCH_3$	L10	Cs_2CO_3	$Pd(S\text{-}BINAP)Cl_2$	63	81
13	$PhCH_3$	L10	Cs_2CO_3	$Pd(PPh_3)_2Cl_2$	65	34
14	$PhCH_3$	L10	Cs_2CO_3	$Pd(dppf)Cl_2$	38	33
15	$PhCH_3$	L10	CsF	$Pd(S\text{-}BINAP)Cl_2$	60	78
16	$PhCH_3$	L10	KOtBu	$Pd(S\text{-}BINAP)Cl_2$	46	61
17	$PhCH_3$	L10	K_2CO_3	$Pd(S\text{-}BINAP)Cl_2$	39	58
18	DMF	L10	Cs_2CO_3	$Pd(S\text{-}BINAP)Cl_2$	ND	0
19	p-xylene	L10	Cs_2CO_3	$Pd(S\text{-}BINAP)Cl_2$	61	73
20	PhCl	L10	Cs_2CO_3	$Pd(S\text{-}BINAP)Cl_2$	45	65
21[d]	$PhCH_3$	L10	Cs_2CO_3	$Pd(S\text{-}BINAP)Cl_2$	65	90
22[e]	$PhCH_3$	L10	Cs_2CO_3	$Pd(S\text{-}BINAP)Cl_2$	55	90



[a]Conditions: **1a** (0.1 mmol), **2a** (0.15 mmol), a catalyst (10 mol %), a ligand (20% mmol), and a base in 2 equiv of solvent (2 mL) at 120 °C for 48 h under Ar. [b]Isolated yield of **3aa**. [c]The ee value was determined by chiral HPLC at 60 and 50 °C.

Downloaded from pubs.acs.org/orlef7/article-pdf/28/40/12587/6693849/acs.orglett.6c03398.pdf by TEXAS TECH UNIV user on 22 October 2026

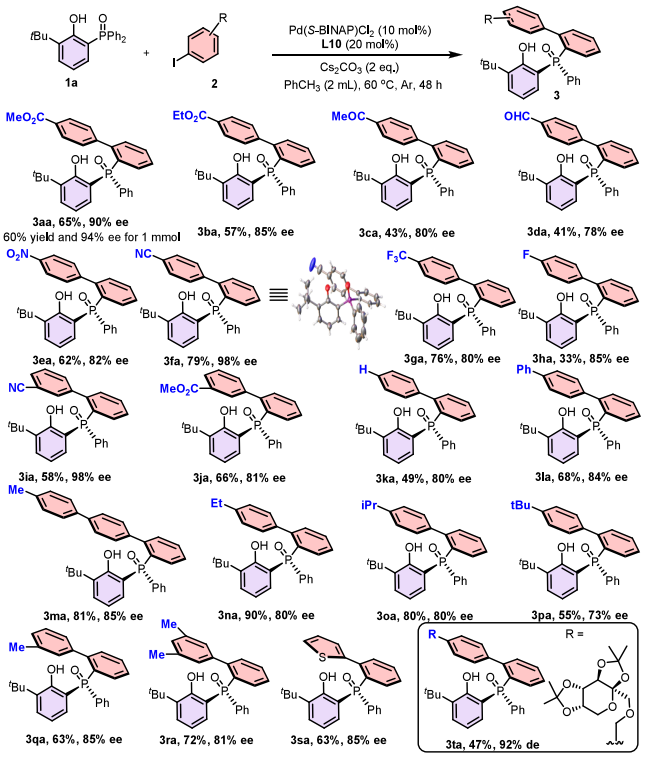
https://doi.org/10.1021/acs.orglett.6c03398
Org. Lett. 2026, 28, 12587−12593

oxazoline ligands (Table 1, entries 4−6) were subsequently evaluated; however, none proved to be superior to the initial system. Notably, our exploration of the catalytic performance of chiral amino acids demonstrates that (*S*)-6-oxopiperidine-2-carboxylic acid (**L10**) can efficiently boost the enantioselectivity of the resultant product and achieve desirable yields simultaneously (Table 1, entries 7−10). Next, with **L10** as the chiral ligand, palladium catalysts such as $Pd(PPh_3)_4$, Pd(*S*-BINAP)Cl_2, $Pd(PPh_3)_2Cl_2$, and Pd(dppf)Cl_2 (Table 1, entries 11−14, respectively) were again evaluated. We found that Pd(*S*-BINAP)Cl_2 can significantly improve stereoselectivity and yield (Table 1, entry 12). Encouraged by this result, we also tried using other bases instead of cesium carbonate to improve the reaction efficiency, but the resulting performance failed to meet our expectations (Table 1, entries 15−17). Subsequently, we hope that different solvents could change the result of the reaction. When DMF, *p*-xylene, and PhCl were used instead of the original solvent (Table 1, entries 18−20, respectively), the yield and ee value of **3aa** were not improved. Further experiments confirmed that appropriately decreasing the temperature can facilitate the conversion of the reaction and increase the ee value (Table 1, entries 21 and 22). Thus, we established the Pd(*S*-BINAP)Cl_2 (10 mol %)/**L10** (20 mol %) optimal catalyst system with 2.0 equiv of Cs_2CO_3 in $PhCH_3$ (2 mL) (Table 1, entry 21).

With the optimal reaction conditions in hand, we then examined the scope of this enantioselective transformation. A broad range of aryl iodides were well tolerated, affording the desired P-stereogenic chiral compounds with excellent yield up to 90% and enantioselectivity up to 98% ee, as summarized in Scheme 2. Initially, various electron-withdrawing groups, including -CO_2Me, -CO_2Et, -COMe, -CHO, NO_2, -CN, -CF_3, and -F, were found to be well tolerated at the *para* position of the benzene ring, affording the target products in good yields with high stereoselectivity (**3aa**−**3ha**, respectively). Meanwhile, we found that the gram-scale synthesis of **3aa** could be carried out without a significant loss of yield or enantioselectivity. Subsequently, under the optimized conditions, the reaction of 4-cyanoiodobenzene with **1a** afforded product **3fa** with excellent enantioselectivity (up to 98% ee), the structure of which was unambiguously confirmed by single-crystal X-ray diffraction analysis (CCDC 2580798). The results show that high stereoselectivity could also be obtained when electron-withdrawing groups (such as -CN and -CO_2Me) are located in the *meta* position of the benzene ring (**3ia** and **3ja**, respectively). The generality of this method was then evaluated with substrates containing electron-donating groups such as -H, -Ph, -*p*-MePh, -Et, -^{i}Pr, and -^{t}Bu at different positions on the benzene ring. These substrates were successfully converted into products **3ka**−**3qa** with high enantioselectivities (>80% ee). Interestingly, a substrate bearing a *m*-dimethyl substitution was also tolerated, affording product **3ra** in 72% yield with 87% ee. Notably, heteroaromatic systems also proved to be suitable substrates for the reaction (**3sa**). We further demonstrated the applicability of this method to natural product-based structure. A chiral pyran derivative featuring a *para*-substituted benzene ring served as a competent substrate, delivering desired product **3ta** with excellent diastereoselectivity.

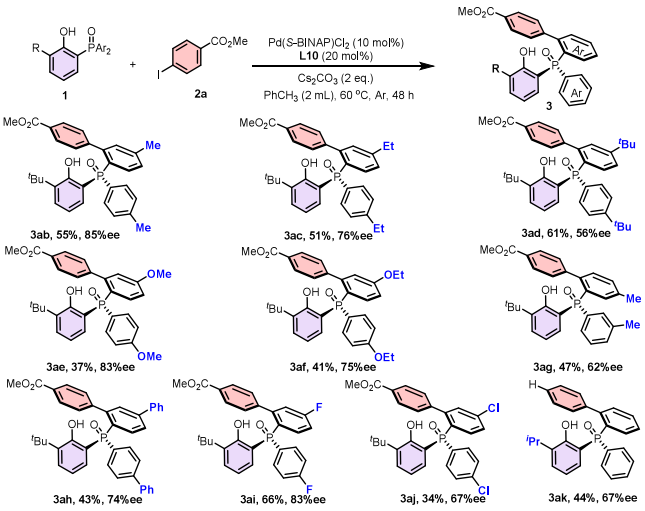
Inspired by these promising results, we continued to explore the efficiency of substrate **2** in achieving asymmetric C−H arylation under the same catalytic system (Scheme 3). First, different substituents on diphenylphosphine oxide were

Scheme 2. Substrate Scope of Aryl Iodides[a−c]



[a]Conditions: **1a** (0.1 mmol), **2** (0.15 mmol), a catalyst (10 mol %), a ligand (20% mmol), and a base (2 equiv) in a solvent (2 mL) at 60 °C for 48 h under Ar. [b]Isolated yield of product **3aa**. [c]The ee value was determined by chiral HPLC.

Scheme 3. Substrate Scope of Diarylphosphine Oxides[a−c]



[a]Conditions: **1** (0.1 mmol), **2a** (0.15 mmol), a catalyst (10 mol %), a ligand (20% mmol), and a base (2 equiv) in a solvent (2 mL) at 60 °C for 48 h under Ar. [b]Isolated yield of product **3aa**. [c]The ee value was determined by chiral HPLC.

screened. The reaction was smoothly facilitated by common electron-donating groups such as -Me, -Et, -^{t}Bu, -OMe, and -OEt, affording the product without compromising the yield or enantioselectivity (**3ab**−**3ag**). Other substituents, including a highly conjugated benzene ring and electron-withdrawing halogen groups, can also be accommodated in the reaction,

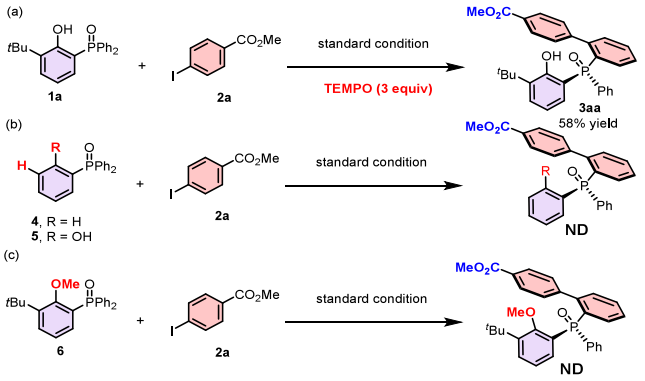
https://doi.org/10.1021/acs.orglett.6c03398
Org. Lett. 2026, 28, 12587−12593

Downloaded from pubs.acs.org/orlef7/article-pdf/28/40/12587/68693849/acs.orglett.6c03398.pdf by TEXAS TECH UNIV user on 22 October 2026

albeit with relatively poor reaction performance (**3ah**−**3aj**). A decrease in enantioselectivity was observed when the *tert*-butyl group was replaced with the less hindered isopropyl group (**3ak**). This inverse correlation indicates that substantial steric bulk on the phenol ring is crucial to achieving high enantioselectivity.

Several control experiments were then carried out to elucidate the reaction mechanism (Scheme 4). When the

Scheme 4. Mechanistic Studies



reaction was conducted under the standard conditions in the presence of radical scavenger TEMPO, the target product was still obtained in 58% yield. This result suggests that a radical process is not operative in this transformation (Scheme 4a). Subsequent experiments confirmed that in the absence of the *tert*-butyl and phenolic hydroxyl groups, triphenylphosphine oxide **4** did not react with compound **2a**, indicating that the phosphoryl group played no role in directing C−H activation. Further experiments, in which compound **5** (lacking the *tert*-butyl substituent) was allowed to react with **2a**, confirmed that the *tert*-butyl group is essential not only for stereoselectivity but also for the overall viability of the reaction (Scheme 4b). Finally, we confirmed the crucial role of phenolic hydroxyl groups in directing C−H bond activation by using compound **6** substituted with methoxy groups instead of **1a** and reacting with **2a** in the reaction (Scheme 4c).

To compare the reactivity of the two phenyl rings in the substrate (the R structure in Figure 2, phenyl rings A and B),

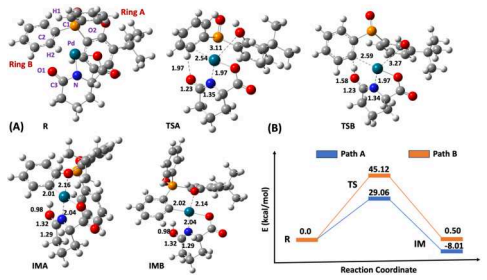


Figure 2. DFT calculations for paths A and B.

we performed density functional theory (DFT) calculations. The first step of the reaction involves bond formation between the palladium (Pd) of the catalyst and a carbon atom on one of the phenyl rings, followed by a hydrogen transfer to the C═O group of the catalyst. The activation can occur through interaction with ring A (path A) or ring B (path B). To determine which pathway is energetically favored, all relevant reactants, intermediates (IM), and transition states (TSs) for both reaction routes were optimized and compared.

In the ring A pathway, the Pd−C1 bond length in the intermediate is 2.01 Å, showing that palladium has formed a bond with the aromatic carbon. This bond becomes longer in the transition state (2.54 Å). At the same time, the hydrogen that participates in the reaction begins to move toward the catalyst's carbonyl group. The O1−H1 distance decreases from 1.97 Å (TSA) to a normal O−H bond length of 0.98 Å in the IMA (Figure 2A). The carbonyl bond (C3═O1) is shorter in TSA than in IMA, while the nearby C3−N bond shows a contrasting behavior. The O2−Pd interactions also weaken during the transition state, stretching from 2.16 to 3.11 Å, which suggests that the palladium center temporarily adjusts its coordination environment as it interacts with the substrate. The ring B pathway shows almost the same pattern. The Pd−C2 bond length is 2.02 Å in IMB and increases to 2.59 Å in TSB, matching the behavior seen for ring A. The hydrogen involved in this pathway also moves toward the catalyst, and the O1−H2 distance decreases from 1.58 to 0.98 Å. Although this TS distance is slightly shorter than the value seen for ring A, it still clearly indicates hydrogen transfer. The carbonyl and C−N bond lengths shift in nearly the same way as they do in the ring A reaction, and the O2−Pd bond again becomes weaker in TSB. Therefore, these structural changes show that both rings follow the same basic reaction pattern. Palladium begins forming a bond with the aromatic carbon, while a hydrogen atom is transferred to the carbonyl group of the catalyst. The small differences we see between the two sets of distances, especially in the transition states, likely explain why one ring is slightly more favorable than the other from an energetic point of view.

The energy results provide (Figure 2B) a clear picture of which phenyl ring is more likely to participate in the reaction. For path A, the activation energy is 29.06 kcal/mol, which is significantly lower than that obtained for path B (45.12 kcal/mol). This large difference, more than 15 kcal/mol, shows that the system requires much less energy to reach the transition state when the reaction occurs on ring A. In other words, Pd−C bond formation and hydrogen transfer are far more accessible along path A. The relative stabilities of the intermediates also support this result. For path A, intermediate IMA lies 8.01 kcal/mol lower in energy than the reactant, indicating that the system becomes more stable once palladium begins to interact with ring A. In contrast, the intermediate for path B is slightly higher in energy than that of the reactant (+0.50 kcal/mol). This means that the formation of IMB is not energetically favorable and does not provide any driving force for the reaction. These results show that path A is clearly the preferred route. It proceeds through a more stable intermediate and requires a much smaller energy barrier to reach the transition state. Path B, with its unfavorable intermediate and substantially higher activation energy, is much less likely to occur under the same reaction conditions. Overall, the energy landscape strongly supports the conclusion that the reaction is initiated on ring A rather than ring B.

It is worth mentioning that paths A and B also correspond to the two competing stereochemical pathways. The formation of IMA yields the *S* configuration, whereas the formation of IMB yields the *R* configuration, as indicated in the caption of Figure 2. Therefore, the much lower activation barrier calculated for path A (29.06 kcal/mol) compared to that for path B (45.12 kcal/mol) is consistent with the experimentally observed

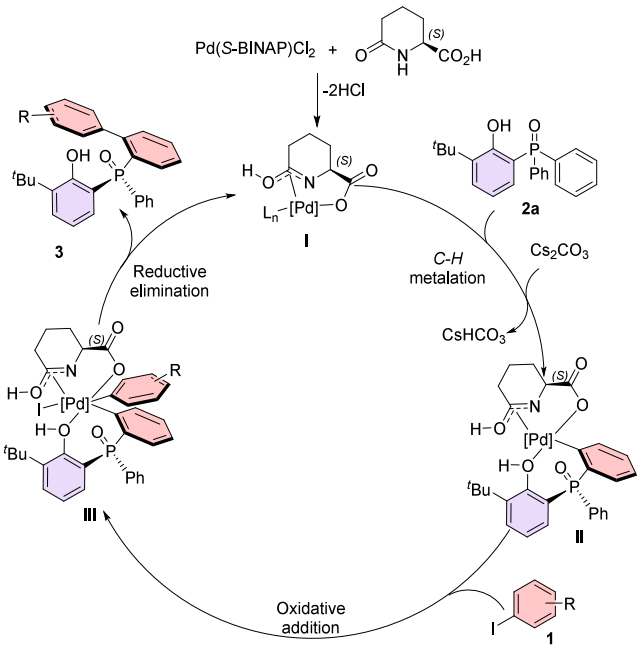
Downloaded from pubs.acs.org/orlef7/article-pdf/28/40/12587/6693849/acs.orglett.6c03398.pdf by TEXAS TECH UNIV user on 22 October 2026

https://doi.org/10.1021/acs.orglett.6c03398
Org. Lett. 2026, 28, 12587−12593

preference for the *S* enantiomer. To better understand the origin of this energy difference, we further performed noncovalent interaction (NCI) analysis for TSA and TSB (Figure S1). The three-dimensional NCI surfaces reveal different interaction environments in the two transition states. TSA shows a broader distribution of favorable weak attractive and van der Waals contacts around the substrate−catalyst interface, whereas TSB displays less attractive regions in the sterically crowded part of the complex. These results suggest that TSA is better accommodated within the chiral catalytic environment, whereas the geometry of TSB introduces greater steric repulsion. The NCI analysis therefore supports the calculated preference for path A and provides a structural explanation of the observed enantioselectivity.

On the basis of mechanistic experiments and references to relevant literature, we propose a possible catalytic cycle mechanism for the phenolic hydroxyl-directed asymmetric C−H arylation (Scheme 5). First, Pd(*S*-BINAP)Cl_2 and (*S*)-6-oxopiperidine-2-carboxylic acid (**L10**) coordinate to form metal complex **I** and then coordinate with -OH group of **2a** and activate the C−H bond at the adjacent position of the benzene ring to form seven-memberied ring intermediate **II**. Then, intermediate **II** and **1** undergo a C−I bond insertion reaction to afford intermediate **III**, and then **III** undergoes a reductive elimination reaction to afford final product **3** and Pd(II) species and completes the catalytic cycle.

Scheme 5. Proposed Catalytic Cycle



In summary, we have developed a convergent and straightforward method for asymmetric catalytic arylation by employing phenolic hydroxyl as a directing group enabling the formation of P-stereogenic chirality. This method utilizes newly synthesized triarylphosphine oxides as a substrate for C(sp^2)−H bond arylation via using aryl iodides, with Pd(*S*-BINAP)Cl_2 identified as the optimal catalyst and commercially available (*S*)-6-oxopiperidine-2-carboxylic acid as a chiral ligand. The substrate scope study demonstrated broad functional group tolerance, delivering enantioselectivity up to 98% ee and yield up to 90% yield across a diverse range of triarylphosphine oxides and aryl iodides, including natural product-based structure chiral pyran. A plausible catalytic cycle was proposed based on experimental results and DFT calculations. Further studies of the application of these new P-stereogenic chiral compounds are underway in our laboratory.

■ ASSOCIATED CONTENT

Data Availability Statement

The data underlying this study are available in the published article and its Supporting Information.

Supporting Information

The Supporting Information is available free of charge at https://pubs.acs.org/doi/10.1021/acs.orglett.6c03398.

General experimental procedures, full spectroscopic data, and copies of ^1H, ^{13}C, ^{31}P, and ^{19}F NMR spectra (PDF)

Accession Codes

Deposition Number 2580798 contains the supplementary crystallographic data for this paper. These data can be obtained free of charge via the joint Cambridge Crystallographic Data Centre (CCDC) and Fachinformationszentrum Karlsruhe Access Structures service.

■ AUTHOR INFORMATION

Corresponding Authors

Shengzhou Jin − *Hubei Key Laboratory of Pollutant Analysis & Reuse Technology, College of Chemistry and Chemical Engineering, Hubei Normal University, Huangshi 435002, China; State Key Laboratory of Coordination Chemistry, Nanjing University, Nanjing 210023, P. R. China;* orcid.org/0009-0006-4484-248X; Email: Jinshengzhou@hbnu.edu.cn

Ruibin Liang − *Department of Chemistry and Biochemistry, Texas Tech University, Lubbock, Texas 79409, United States;* orcid.org/0000-0001-8741-1520; Email: rliang@ttu.edu

Guigen Li − *School of Pharmacy, Continuous Flow Engineering Laboratory of National Petroleum and Chemical Industry, Changzhou University, Changzhou, Jiangsu 213164, China; School of Chemistry and Chemical Engineering, Nanjing University, Nanjing 210023, China;* orcid.org/0000-0002-9312-412X; Email: guigenli@nju.edu.cn

Authors

Mohammad Khavani − *Department of Chemistry and Biochemistry, Texas Tech University, Lubbock, Texas 79409, United States*

Yu Wang − *School of Chemistry and Chemical Engineering, Nanjing University, Nanjing 210023, China*

Ankit Pandey − *Department of Chemistry and Biochemistry, Texas Tech University, Lubbock, Texas 79409, United States*

Qiyang Jiang − *Hubei Key Laboratory of Pollutant Analysis & Reuse Technology, College of Chemistry and Chemical Engineering, Hubei Normal University, Huangshi 435002, China*

Sai Zhang − *School of Pharmacy, Continuous Flow Engineering Laboratory of National Petroleum and Chemical Industry, Changzhou University, Changzhou, Jiangsu 213164, China;* orcid.org/0009-0004-0826-9650

https://doi.org/10.1021/acs.orglett.6c03398
Org. Lett. 2026, 28, 12587−12593

Downloaded from pubs.acs.org/orlef7/article-pdf/28/40/12587/68693849/acs.orglett.6c03398.pdf by TEXAS TECH UNIV user on 22 October 2026

Complete contact information is available at:
https://pubs.acs.org/10.1021/acs.orglett.6c03398

Author Contributions

[▽]S.J., M.K., and Y.W. contributed equally to this work.

Notes

The authors declare no competing financial interest.

■ ACKNOWLEDGMENTS

This work was supported by the Texas University Fund (TUF) for the Human Molecular Aging Center at Texas Tech University under internal Grant TUF6656 and by the Robert A. Welch Foundation (Grant D-2108-20220331).

■ REFERENCES

(1) (a) Dai, Q.; Li, W.; Li, Z.; Zhang, J. P-Chiral Phosphines Enabled by Palladium/Xiao-Phos-Catalyzed Asymmetric P-C Cross-Coupling of Secondary Phosphine Oxides and Aryl Bromides. *J. Am. Chem. Soc.* **2019**, *141*, 20556−20564. (b) Pang, L.; Sun, Q.; Huang, Z.; Li, G.; Liu, J.; Guo, J.; Yao, C.; Yu, J.; Li, Q. Palladium-Catalyzed Stereoselective Cleavage of C-P Bond: Enantioselective Construction of Atropisomers Containing a P-Stereogenic Center. *Angew. Chem., Int. Ed.* **2022**, *61*, 12253−12258. (c) Zhao, D.; Sun, J.; Chen, N.; Ge, Y.; Liu, J.; Bai, L.; Luan, X. Catalytic Asymmetric P-Site Dearomatization Enables Kinetic Resolution. *J. Am. Chem. Soc.* **2025**, *147*, 23202−23212. (d) Wang, W. H.; Zhang, S. Y.; Zhang, Y. X.; Wang, Y. Q.; Zhang, Q. W. Nickel-Catalyzed Asymmetric Synthesis of Ambiphilic Secondary Phosphine Oxides. *J. Am. Chem. Soc.* **2025**, *147*, 14797−14805.

(2) Knowles, W. S.; Sabacky, M. J.; Vineyard, B. D.; Weinkauff, D. J. Asymmetric Hydrogenation with a Complex of Rhodium and a Chiral Bisphosphine. *J. Am. Chem. Soc.* **1975**, *97*, 2567−2568.

(3) (a) Forbes, K. C.; Jacobsen, E. N. Enantioselective hydrogen-bond-donor catalysis to access diverse stereogenic-at-P(V) compounds. *Science.* **2022**, *376*, 1230−1236. (b) Zhang, L.; Wang, M.; Luo, Y.; Zhang, Z.; Liu, D.; Zhang, W. Asymmetric Synthesis of Diverse P(V) Compounds Bearing a C-P Bond via Desymmetrization of Phosphonic Dichlorides Catalyzed by a Chiral Bicyclic Imidazole. *J. Am. Chem. Soc.* **2025**, *147*, 47712−47721. (c) Liu, W.; Ling, Z.; Liu, Y. Z.; Deng, W.-P. Catalytic asymmetric construction of remote P or other heteroatom (Si/S) stereogenic axially chiral scaffolds. *Chem. Sci.* **2026**, *17*, 240−246.

(4) (a) Knouse, K. W.; deGruyter, J. N.; Schmidt, M. A.; Zheng, B.; Vantourout, J. C.; Kingston, C.; Mercer, S. E.; Mcdonald, I. M.; Olson, R. R.; Zhu, Y.; Hang, C.; Zhu, J.; Yuan, C.; Wang, Q.; Park, P.; Eastgate, M. D.; Baran, P. S. Unlocking P(V): Reagents for chiral phosphorothioate synthesis. *Science* **2018**, *361*, 1234−1238. (b) Qi, Z. C.; Li, Y.; Wang, J.; Ma, L.; Wang, G. W.; Yang, S. D. Electrophilic Selenium-Catalyzed Desymmetrizing Cyclization to Access P-Stereogenic Heterocycles. *ACS Catal.* **2023**, *13*, 13301−13309. (c) Fang, S. S.; Hu, X. J.; Li, M. H.; Qi, S.; Xie, T.; Wang, J. B.; Yao, H. Q.; Zhang, J.; Zhang, J. H.; Zhu, L.; Shang, M. Ligand-Enabled Cu-Catalyzed Stereoselective Synthesis of P-Stereogenic ProTides. *J. Am. Chem. Soc.* **2024**, *146*, 31339−31347. (d) Che, F.; Hu, J.; Liao, M.; Luo, Z.; Long, H.; Li, B.; Chi, Y. R.; Wu, X. Synthesis of P(V)-Stereogenic Phosphorus Compounds via Organocatalytic Asymmetric Condensation. *J. Am. Chem. Soc.* **2024**, *146*, 33763−33773. (e) Yao, H. Q.; Cai, Y. M.; Xie, T.; Lv, J. Y.; Fang, S. S.; Li, M. H.; Shang, M. Modular Access to P(V)-Stereogenic Compounds via Cu-Catalyzed Desymmetrization of (Thio)Phosphonic Dichlorides. *Angew. Chem., Int. Ed.* **2025**, *64*, No. e202509807. (f) Che, F.; Hu, J.; Li, B.; Wang, Y.; Wu, X.; Chi, Y. R. Asymmetric Organocatalytic Methylation of Prochiral Phosphinic Acids: Construction of P(V)-Stereogenic Centers. *ACS Catal.* **2025**, *15*, 20184−20193. (g) Ren, S. M.; Yang, W. J.; Ding, K.; Kang, J.; Zou, J. X.; Su, B. Dynamic Kinetic Asymmetric P-C Coupling of Secondary Phosphine Oxides with Alkenyl Iodides. *Org. Lett.* **2025**, *27*, 6082−6087. (h) Zhu, D. Y.; Zhang, Y. T.; Cheng, F.; Kong, Q.; Dang, H. X.; Jiao, H. J.; Zhang, Y.; Zhang, X. M.; Wang, S. H.; Li, S. Y. Enantio- and Diastereoselective Synthesis of P-Stereogenic Phospholane Oxides via Cobalt-Catalyzed Hydroalkylation. *Org. Lett.* **2025**, *27*, 4251−4256. (i) Wan, B.; Castiñeira Reis, M.; Ramspoth, T. F.; Harutyunyan, S. R. Manganese(I)-Catalyzed Enantioselective Alkylation To Access P-Stereogenic Phosphines. *J. Am. Chem. Soc.* **2025**, *147*, 3740−3746. (j) Lavrencic, L.; Dhawa, U.; Hu, X. Nickel-Hydride-Catalyzed Hydroalkylation of Cyclic Phosphinates: Generation of Enantioenriched Phosphorus and Carbon Stereocenters. *ACS Catal.* **2025**, *15*, 16018−16025. (k) Hu, H. L.; Fang, S.; Luo, X.; He, J.; Wu, J. H.; Su, Z.; Xu, Z.; Wang, T. Organocatalytic Enantioselective Arylation to Access Densely Aryl-Substituted P-Stereogenic Centers. *Org. Lett.* **2025**, *27*, 109−114. (l) Daniels, B. S.; Blackburn, B. G.; Scribner, S. J.; Dong, V. M. Pathway to P(V)-Stereogenic Phosphoramidates by Enantioselective Yttrium Catalysis. *J. Am. Chem. Soc.* **2025**, *147*, 21339−21346. (m) Zheng, G. L.; Zhang, Y.; Zhang, J. M.; Chen, L.; Xue, X. S.; He, Z. T. Stereogenic P(V) Synthesis via Catalytic Continuous Substitutions. *J. Am. Chem. Soc.* **2025**, *147*, 13566−13576.

(5) (a) Han, Z. S.; Zhang, L.; Xu, Y.; Sieber, J. D.; Marsini, M. A.; Li, Z.; Reeves, J. T.; Fandrick, K. R.; Patel, N. D.; Desrosiers, J.-N.; Qu, B.; Chen, A.; Rudzinski, D. M.; Samankumara, L. P.; Ma, S.; Grinberg, N.; Roschangar, F.; Yee, N. K.; Wang, G.; Song, J. J.; Senanayake, C. H. Efficient Asymmetric Synthesis of Structurally Diverse P-Stereogenic Phosphinamides for Catalyst Design. *Angew. Chem., Int. Ed.* **2015**, *54*, 5474−5477. (b) Yang, G.-H.; Li, Y.; Li, X.; Cheng, J.-P. Access to P-chiral phosphine oxides by enantioselective allylic alkylation of bisphenols. *Chem. Sci.* **2019**, *10*, 4322−4327. (c) Liu, X.-T.; Zhang, Y.-Q.; Han, X.-Y.; Sun, S.-P.; Zhang, Q.-W. Ni-Catalyzed Asymmetric Allylation of Secondary Phosphine Oxides. *J. Am. Chem. Soc.* **2019**, *141*, 16584−16589. (d) Zhu, R.-Y.; Chen, L.; Hu, X.-S.; Zhou, F.; Zhou, J. Enantioselective synthesis of P-chiral tertiary phosphine oxides with an ethynyl group via Cu(i)-catalyzed azide-alkyne cycloaddition. *Chem. Sci.* **2020**, *11*, 97−106. (e) Li, Y.-B.; Tian, H.; Yin, L. Copper(I)-Catalyzed Asymmetric 1,4-Conjugate Hydrophosphination of α,β-Unsaturated Amides. *J. Am. Chem. Soc.* **2020**, *142*, 20098−20106. (f) Genov, G. R.; Douthwaite, J. L.; Lahdenperä, A. S. K.; Gibson, D. C.; Phipps, R. J. Enantioselective remote C-H activation directed by a chiral cation. *Science* **2020**, *367*, 1246−1251. (g) Hu, P.; Kong, L.; Wang, F.; Zhu, X.; Li, X. Twofold C-H Activation-Based Enantio- and Diastereoselective C-H Arylation Using Diarylacetylenes as Rare Arylating Reagents. *Angew. Chem., Int. Ed.* **2021**, *60*, 20424−20429. (h) Wang, C.; Huang, K.; Ye, J.; Duan, W.-L. Asymmetric Synthesis of P-Stereogenic Secondary Phosphine-Boranes by an Unsymmetric Bisphosphine Pincer-Nickel Complex. *J. Am. Chem. Soc.* **2021**, *143*, 5685−5690.

(6) (a) Nishida, G.; Noguchi, K.; Hirano, M.; Tanaka, K. Enantioselective Synthesis of P-Stereogenic Alkynylphosphine Oxides by Rh-Catalyzed [2+2+2] Cycloaddition. *Angew. Chem., Int. Ed.* **2008**, *47*, 3410−3413. (b) Ma, Y. N.; Li, S. X.; Yang, S. D. New Approaches for Biaryl-Based Phosphine Ligand Synthesis via P=O Directed C-H Functionalizations. *Acc. Chem. Res.* **2017**, *50*, 1480−1492. (c) Sun, Y.; Cramer, N. Rhodium(III)-Catalyzed Enantiotopic C-H Activation Enables Access to P-Chiral Cyclic Phosphinamides. *Angew. Chem., Int. Ed.* **2017**, *56*, 364−367. (d) Trost, B. M.; Spohr, S. M.; Rolka, A. B.; Kalnmals, C. A. Desymmetrization of Phosphinic Acids via Pd-Catalyzed Asymmetric Allylic Alkylation: Rapid Access to P-Chiral Phosphinates. *J. Am. Chem. Soc.* **2019**, *141*, 14098−14103. (e) Ye, J.; You, Y.; Xu, D.; Deng, S.; Qi, L.; Liu, C.; Liu, C. C.; Cong, H.; Wang, P.; Cheng, H. G.; Zhou, Q. Construction of P-Stereogenic Centers via Palladium/Chiral Norbornene Cooperative Catalysis-Enabled Desymmetrization and Kinetic Resolution. *CCS Chem.* **2025**, *7*, 3025−3035. (f) Zhang, C. W.; Hu, X. Q.; Yan, S. Y.; Xiong, J. Q.; Duan, W. L. Chiral Amide-Enabled Cobalt-Catalyzed Enantioselective C-H Annulation for the Synthesis of P-Stereogenic Arylphosphinamides. *Org. Lett.* **2026**, *28*, 9926−9931. (g) Platt, F. M.; Prindl, M. I.; Zhou, Z.; Cordes, D. B.; Panchal, H.; Smith, A. D. Controlling phosphorus-stereogenicity organocatalytic acylative desymmetrisation of bisphenols. *Chem. Sci.* **2026**, DOI: 10.1039/D6SC05320C. (h) Sau,

Downloaded from pubs.acs.org/orlef7/article-pdf/28/40/12587/6693849/acs.orglett.6c03398.pdf by TEXAS TECH UNIV user on 22 October 2026

S.; Ali, A.; Pradhan, K.; Naskar, P.; Gandon, V.; Sahoo, A. K. Desymmetrization and Atroposelective Cobalt Catalyzed C-H Annulation of Phosphinic Amides with Ynamides. *Org. Lett.* **2026**, *28*, 3236−3242.
(7) (a) Kuang, X.; Li, J. J.; Liu, T.; Ding, C. H.; Wu, K.; Wang, P.; Yu, J. Q. Cu-mediated enantioselective C-H alkynylation of ferrocenes with chiral BINOL ligands. *Nat. Commun.* **2023**, *14*, 7698. (b) Li, J. J.; Zeng, X. X.; Kuang, X.; Shen, H. C.; Wang, P.; Yu, J. Q. Atroposelective Diverse Remote *meta*-C-H Functionalization via Kinetic Resolution. *J. Am. Chem. Soc.* **2025**, *147*, 6594−6603. (c) Li, Y. H.; Ouyang, Y.; Yan, J. L.; Chekshin, N.; Yu, J. Q. From Mono-*N*-Protected Amino Acids to Pyridones: A Decade of Evolution of Bifunctional Ligands for Pd(II)-Catalyzed C-H Activation. *Acc. Chem. Res.* **2025**, *58*, 2910−2926.
(8) Du, Z. J.; Guan, J.; Wu, G. J.; Xu, P.; Gao, L. X.; Han, F. S. Pd(II)-Catalyzed Enantioselective Synthesis of P-Stereogenic Phosphinamides via Desymmetric C-H Arylation. *J. Am. Chem. Soc.* **2015**, *137*, 632−635.
(9) (a) Haines, B. E.; Yu, J.-Q.; Musaev, D. G. Enantioselectivity Model for Pd-Catalyzed C-H Functionalization Mediated by the Mono-N-protected Amino Acid (MPAA) Family of Ligands. *ACS Catal.* **2017**, *7*, 4344−4354. (b) Shao, Q.; Wu, K.; Zhuang, Z.; Qian, S.; Yu, J.-Q. From $Pd(OAc)_2$ to Chiral Catalysts: The Discovery and Development of Bifunctional Mono-*N*-Protected Amino Acid Ligands for Diverse C-H Functionalization Reactions. *Acc. Chem. Res.* **2020**, *53*, 833−851.
(10) Song, S. Y.; Li, Y.; Ke, Z.; Xu, S. Iridium-Catalyzed Enantioselective C-H Borylation of Diarylphosphinates. *ACS Catal.* **2021**, *11*, 13445−13451.
(11) Hu, P.; Kong, L.; Wang, F.; Zhu, X.; Li, X. Twofold C−H Activation-Based Enantio-and Diastereoselective C-H Arylation Using Diarylacetylenes as Rare Arylating Reagents. *Angew. Chem., Int. Ed.* **2021**, *60*, 20424−20429.
(12) Yao, Q. J.; Chen, J. H.; Song, H.; Huang, F. R.; Shi, B. F. Cobalt/Salox-Catalyzed Enantioselective C-H Functionalization of Arylphosphinamides. *Angew. Chem., Int. Ed.* **2022**, *61*, No. e202202892.
(13) Zhou, G.; Chen, J. H.; Yao, Q. J.; Huang, F. R.; Wang, Z. K.; Shi, B. F. Base-Promoted Electrochemical Co(II)-catalyzed Enantioselective C-H Oxygenation. *Angew. Chem., Int. Ed.* **2023**, *62*, No. e202302964.
(14) Lin, Y.; von Münchow, T.; Ackermann, L. Cobaltaelectro-Catalyzed C-H Annulation with Allenes for Atropochiral and P-Stereogenic Compounds: Late-Stage Diversification and Continuous Flow Scale-Up. *ACS Catal.* **2023**, *13*, 9713−9723.
(15) Das, A.; Mandal, R.; Ravi Sankar, H. S.; Kumaran, S.; Premkumar, J. R.; Borah, D.; Sundararaju, B. Reversal of Regioselectivity in Asymmetric C-H Bond Annulation with Bromoalkynes under Cobalt Catalysis. *Angew. Chem., Int. Ed.* **2024**, *63*, No. e202315005.
(16) (a) Zhou, T.; Fan, L. J.; Chen, Z. J.; Jiang, M. X.; Qian, P. F.; Hu, X.; Zhang, K.; Shi, B. F. Synthesis of P-Stereogenic Phosphinamides via Pd(II)-Catalyzed Enantioselective C-H Alkynylation. *Org. Lett.* **2023**, *25*, 5724−5729. (b) Chen, Z. J.; Fan, L. J.; Xie, P. P.; Qian, P. F.; Hu, X.; Zhou, T.; Shi, B. F. Pd(II)-Catalyzed enantioselective C-H olefination toward the synthesis of P-stereogenic phosphinamides. *Chem. Commun.* **2024**, *60*, 1623−1626.
(17) Jin, S.; Wang, Y.; Yan, J. X.; Xu, T.; Ning, M.; Yuan, Q.; Li, G. $P(=O)R_2$-Directed Asymmetric Catalytic C-H Olefination Leading to C-N Axially Chiral Targets. *Org. Lett.* **2025**, *27*, 2838−2844.

Downloaded from pubs.acs.org/orlef7/article-pdf/28/40/12587/6869849/acs.orglett.6c03398.pdf by TEXAS TECH UNIV user on 22 October 2026

https://doi.org/10.1021/acs.orglett.6c03398
Org. Lett. 2026, 28, 12587−12593